Regulation of Cortical Actin Cytoskeleton Assembly during Polarized Cell Growth in Budding Yeast

Rong Li,* Yi Zheng,‡ and David G. Drubin*

*Department of Molecular and Cell Biology, University of California, Berkeley, California 94720; and ‡Department of Pharmacology, Cornell University, Ithaca, New York 14853

Abstract. We have established an in vitro assay for assembly of the cortical actin cytoskeleton of budding yeast cells. After permeabilization of yeast by a novel procedure designed to maintain the spatial organization of cellular constituents, exogenously added fluorescently labeled actin monomers assemble into distinct structures in a pattern that is similar to the cortical actin distribution in vivo. Actin assembly in the bud of small-budded cells requires a nucleation activity provided by protein factors that appear to be distinct from the barbed ends of endogenous actin filaments. This nucleation activity is lost in cells that lack either Sla1 or Sla2, proteins previously implicated in cortical actin cytoskeleton function, suggesting a possible role for these proteins in the nucleation reaction. The rate and the extent of actin assembly in the bud are increased in permeabilized Δ*cap2* cells, providing evidence that capping protein regulates the ability of the barbed ends of actin filaments to grow in yeast cells. Actin incorporation in the bud can be stimulated by treating the permeabilized cells with GTP-γS, and, significantly, the stimulatory effect is eliminated by a mutation in *CDC42*, a gene that encodes a Rho-like GTP-binding protein required for bud formation. Furthermore, the lack of actin nucleation activity in the *cdc42* mutant can be complemented in vitro by a constitutively active Cdc42 protein. These results suggest that Cdc42 is closely involved in regulating actin assembly during polarized cell growth.

THE establishment of cell polarity is crucial for many biological processes, including embryonic development, neurite outgrowth, cell locomotion, and cell division. A large body of evidence has demonstrated that in many cases, actin, being the principal cytoskeletal component underlying the plasma membrane, provides the structural basis for cell morphogenesis and cell polarity development (Bretscher, 1991). During cell polarization, extracellular signals or endogenous cues first provide instructions to change cell surface morphology. Cells then respond to these signals and initiate structural rearrangements that require actin reorganization at the cell surface. Therefore, determining the mechanisms that control actin dynamics is central to understanding many morphogenetic processes.

The assembly and disassembly of actin are modulated by many cellular factors. By nucleating, cross linking, capping, and severing actin polymers as well as modulating the availability of actin monomers, these factors are able to control the length, stability, and distribution of actin filaments (Stossel et al., 1985, Pollard and Cooper, 1986). Because actin rearranges rapidly in response to a variety of stimuli, it is almost certain that some actin-binding proteins are direct targets of the signal transduction machinery. Studies in tissue culture cells have indicated that GTP-binding proteins play important roles in regulating changes in cytoskeletal organization. For example, the stimulation of actin polymerization that occurs during neutrophil activation is sensitive to pertussis toxin, an inhibitor of heterotrimeric G proteins (Shefcyk et al., 1985), and microinjection of small GTP-binding proteins Rac and Rho into fibroblasts induces membrane ruffling and stress fiber formation, respectively (Ridley and Hall, 1992; Ridley et al., 1992). However, the molecular pathways that connect GTP-binding proteins to the reorganization of the actin cytoskeleton have not been elucidated.

The budding yeast *Saccharomyces cerevisiae* exhibits polarized cell growth during budding and in response to mating factors. Major actin rearrangements occur during these processes: cortical actin patches accumulate at, and actin cables orient toward, the sites of surface growth, namely the bud (Kilmartin and Adams, 1984) and the mating projection (Ford and Pringle, 1986). A large number of genes that are required for polarized growth have been characterized, and the phenotypes and the genetic interactions of the mutant alleles of these genes have been studied extensively (reviewed in Welch et al., 1994). Genes that function in bud formation can be grouped into three classes: those required for bud site selection (*RSR1*, *BUD2-5*, etc.) (Bender and Pringle, 1989; Chant et al., 1991; Chant and Herskowitz, 1991),

Address all correspondence to David G. Drubin, 455 Life Science Addition, Department of Molecular and Cell Biology, University of California, Berkeley, California 94720. Tel.: (510) 642-3692. Fax: (510) 643-6791.

those required for bud site assembly (*CDC24*, *CDC42*, etc.) (Sloat et al., 1981; Johnson and Pringle, 1990), and those that encode the structural components of the cytoskeleton (*ACT1*, *ABP1*, etc.) (Shortle et al., 1982; Drubin et al., 1988). Many of these genes encode polypeptides with sequence homology to mammalian proteins. For example, *CDC42* encodes a Rho-like GTP-binding protein (Johnson and Pringle, 1990), whereas the product of *SLA2* contains a domain homologous to mammalian talin (Holtzman et al., 1993), a protein found in structures that link the actin cytoskeleton to the plasma membrane. Therefore, analysis of polarized cell growth and cytoskeleton assembly in yeast may reveal mechanisms that are common to all eukaryotic organisms.

While genetic analysis of mutant interactions can provide clues about which gene products function together, this level of analysis will not reveal the underlying biochemical mechanisms. Further understanding requires in vitro experiments in which the biochemical basis of genetic interactions can be determined. In this paper, we report the establishment of the first in vitro assay for polarized assembly of the cortical actin cytoskeleton in yeast. After permeabilization of yeast cells by a novel procedure designed to maintain the polarity of cellular constituents, exogenously added fluorescently labeled actin monomers assemble into distinct patches mainly in the bud. This pattern of actin assembly is similar to actin organization in vivo. The kinetics of actin incorporation into the permeabilized cells suggests that an actin nucleation activity must be present to promote actin assembly in the bud. This nucleation activity does not appear to come from the barbed ends of endogenous actin filaments, and it is abolished by mutations in either *SLA1* or *SLA2*, two genes that encode components of the cortical actin cytoskeleton (Holtzman et al., 1993). Furthermore, by analyzing yeast mutants using the permeabilized cell assay, we present evidence that Cdc42, a Rho-like GTP-binding protein required for budding, plays a direct role in regulating actin assembly during polarized cell growth.

Materials and Methods

Strains and Media

Yeast strains used in this work are listed in Table I. Media for yeast growth were the same as described in Sherman et al. (1974).

Protein Purification and Fluorescent Labeling

Actin was purified from frozen rabbit muscle as described (Pardee and Spudich, 1982), and it was stored at −80°C in G buffer (5 mM Tris-HCl, pH 8.0, 0.2 mM ATP, 0.2 mM $CaCl_2$, and 0.2 mM DTT). Filamentous actin was prepared and labeled with *N*-hydroxysuccinimidyl 5-carboxytetramethyl rhodamine (Molecular Probes, Inc., Eugene, OR) as described by Kellogg et al. (1988). Rhodamine actin (Rd-actin)[1] was stored at 2 mg/ml in G buffer at −80°C. An aliquot of Rd-actin was thawed overnight at 4°C and was clarified by centrifugation at 300,000 *g* for 30 min. Rd-actin shows polymerization kinetics similar to unlabeled actin (not shown). Pyrene-labeled actin was prepared as described in Moon et al. (1993). Yeast actin was prepared as described (Holtzman et al., 1994).

The conversion of ATP-actin to ADP-actin using hexokinase (Sigma Immunochemicals, St. Louis, MO) in the presence of glucose was carried out as described (Symons and Mitchison, 1991). As a control for impurities in the hexokinase preparation, glucose was not included in one reaction. The actin from the control reaction behaves similarly to untreated ATP-actin.

1. *Abbreviations used in this paper*: CD, cytochalasin D; GST, glutathione-*S*-transferase; RD-actin, rhodamine-actin.

Table I. Strain List

Strains	Genotype	Source
DDY180	*a ura3-52 his4-619*	Drubin lab
DDY495	*a ura3-52 leu2-3,112 Δsla1::URA3*	Drubin lab
DDY496	*a ura3-52 leu2-3,112 Δsla2::URA3*	Drubin lab
DDY217	*a ura3-52 leu2-3,112 lys2 his3 trp1 Δsac6::URA3*	Drubin lab
DDY262	*a ura3-52 leu2-3,112 lys2 ade2-1 Δabp1::URA3*	Drubin lab
JC93	*a ade2-1 his3-11,15 leu2-3, 112 trp1-1 ura3-1 CAP2*	J. Cooper
JC108	*a ade2-1 his3-11,15 leu2-3, 112 trp1-1 ura3-1 Δcap2::HIS3*	J. Cooper
DRL165-2a	*a ura3-52 leu2-3,112 cdc42-1*	This work
DRL165-5a	*a ura3-52 leu2-3,112*	This work

All of the strains listed above are in S288c background, except that JC93 and JC108 are two congenic strains obtained from J. Cooper (Dept. of Cell Biology and Physiology, Washington University School of Medicine, St. Louis, MO).

The wild-type Cdc42-glutathione-*S*-transferase (GST) fusion protein was expressed in baculovirus-infected insect cells as described in Zheng et al. (1994). To generate $Cdc42^{L61}$ mutant protein, the glutamic acid (codon CAA) at amino acid position 61 was changed to leucine (codon CTA) by site-directed mutagenesis (Sculptor™ in vitro mutagenesis system; Amersham Corp., Arlington Heights, IL). The GST-$Cdc42^{L61}$ fusion protein was expressed following the same procedure as described for the wild-type Cdc42 protein. The GST part from both fusion proteins was cleaved by thrombin digestion. Thrombin was subsequently removed by incubation with *p*-aminobenzoamidine-agarose beads (Sigma). The Cdc42 and $Cdc42^{L61}$ proteins were stored in a buffer containing 20 mM Tris-HCl, pH 8.0, 100 mM NaCl, 10 mM $MgCl_2$, and 2% glycerol at 4°C for up to 2 wk. The resulting wild-type Cdc42 protein was mostly GDP bound, whereas 80% of the $Cdc42^{L61}$ protein was in the GTP bound form, as determined by HPLC analysis (Zheng, Y., and R. Cerione, unpublished results).

Permeabilization of Yeast Cells and In Vitro Actin Assembly

25-ml yeast cultures were grown to ~5 × 10^6 cells/ml. Cells were harvested by centrifugation at 2,000 rpm for 5 min at room temperature. The pellet was washed immediately with 1.0 ml of a cold buffer that consists of 0.5× U buffer (1× U buffer = 50 mM KHepes, pH 7.5, 100 mM KCl, 3 mM $MgCl_2$, and 1 mM EGTA) and 0.5× synthetic dextrose (Sherman et al., 1974). After spinning for 2 s in a microfuge, the supernatant was aspirated as thoroughly as possible, and the pellet was frozen immediately in liquid nitrogen. The cell pellet was next thawed at room temperature and 100 μl of cold U buffer containing 10% glycerol was immediately added. The resulting cell suspension was divided into aliquots, frozen in liquid nitrogen, and stored at −80°C for ≤1 mo. An aliquot was thawed immediately before each actin assembly experiment. 2 μl of the cell suspension was added to 18 μl of U buffer containing 0.5 mg/ml saponin (Sigma) and 1× PI (0.5 mg/ml of each of antipain, leupeptin, pepstatin A, chymostatin, aprotinin, and 1 mM PMSF), and was incubated in U buffer for 30 min at the room temperature. Cells were pelleted, washed with 1 ml of cold U buffer containing PI, and resuspended in 19 μl of U buffer containing 1 mM ATP. The polymerization reaction was initiated by the addition of 1 μl of Rd-actin (20× of the final reaction concentration diluted in G buffer). The reaction was incubated at 25°C in the dark for specified periods and was stopped by the addition of 2.7 μl of 37% formaldehyde (Fisher Scientific, Pittsburgh, PA). When fluorescein dextran was used as a marker for permeability, 1 μl of 10 mg/ml 70 kD fluorescein dextran (Molecular Probes) was added to the cells at the same time as Rd-actin addition. At the end of the polymerization reaction, the cells were pelleted, the supernatant was removed, and the cells were resuspended in U buffer containing ATP and 5% formaldehyde. This procedure does not change the level of Rd-actin incorporation. After a 20-min fixation, the cells were washed two times in U buffer, resuspended in 25 μl U buffer, and pipetted onto a polylysine-

(Sigma) coated slide. After a 5-min incubation in the dark, excess cells were aspirated and the slide was air dried. The slide was washed three times in U buffer, and a drop of mounting solution (Pringle et al., 1989) was added. The slide was covered with a glass coverslip and sealed with nail polish.

Pyrene Actin Assembly Assay

Coassembly of actin or Rd-actin with pyrene-labeled actin was assayed as described in Moon et al. (1993). The assembly condition was 50 mM KHepes, pH 7.5, 100 mM KCl, 3 mM $MgCl_2$, 1 mM EGTA, and 1 mM ATP at 25°C. Pyrene fluorescence was measured in a fluorometer (F-4010; Hitachi Scientific Instruments, Mountain View, CA) with a neutral density filter to minimize bleaching. The excitation wave length was 365 nm, and emission wave length was 407 nm.

Inhibitor, Chemical, and Enzyme Treatments

α Factor (Sigma) was dissolved in DMSO at 5 mg/ml and stored at 4°C. To cause a G1 arrest in ≥95% of the cells, cell cultures at a density of 2.5×10^6 cells/ml were treated with 2.5 μg/ml α factor for 2 h at 30°C or 3 h at 25°C. In the experiment in which permeabilized cells were prepared from successive cell cycle stages, cells were treated with 0.1 μg/ml α factor for 1 h at 30°C to achieve a G1 arrest without mating projection formation.

Cytochalasin D (Sigma) was dissolved in 50% DMSO at 0.5 mM and stored at −20°C.

GTP-γS, GDP-βS, GTP, and ATP-γS were purchased from Boehringer Mannheim Biochemicals (Indianapolis, IN). Permeabilized cells were incubated in U buffer containing PI and 0.2 mM of one of the above nucleotides for 40 min at 30°C. Cells were washed with U buffer before initiating the actin polymerization reactions.

Trypsin and trypsin inhibitor were purchased from Boehringer Mannheim Biochemicals. Cells were incubated in U buffer containing 50 μg/ml trypsin for 30 min at 25°C. At the end of the treatment, 100 μg/ml trypsin inhibitor was added. In the meantime, 50 μg/ml trypsin and 100 μg/ml trypsin inhibitor were added simultaneously to the control cells that had been incubated in U buffer for 30 min at 25°C. The treated cells and the control cells were then washed 2× with cold PI-containing U buffer before proceeding to the next step.

Protein Analysis

Protein concentrations were determined as described by Lowry et al. (1951).

Fluorescence Staining of Cellular Actin

Cells were fixed in yeast extract peptone dextrose media or U buffer containing 5% formaldehyde for 1.5 h at 25°C. Zymolyase treatment and actin immunofluorescence using a rabbit antiactin primary antibody (Drubin et al., 1988) and an FITC-conjugated goat anti-rabbit secondary antibody (Cappel Laboratories, Cochranville, PA) was carried out as described (Moon et al., 1993). Fixed cells were also stained with fluorescein-conjugated phalloidin (Molecular Probes) as described (Pringle et al., 1989).

Fluorescence Microscopy

Fluorescence imaging was performed either on a microscope (Axioskop; Carl Zeiss, Inc., Thornwood, NY) with a HB100 W/Z high pressure mercury lamp and a Zeiss 100× Plan Neofluar oil immersion objective (for photography), or on a Nikon inverted microscope with a Nikon 100× Plan Neofluar oil immersion objective (for fluorescence quantification).

Fluorescence Quantification and Data Analysis

Fluorescence images were displayed (software by Perceptics Biovision, Knoxville, TN) on a Mac IIx computer. The average fluorescence intensity in specific regions of the cell (i.e., the bud or the mother cell) was measured using the National Institute of Health Image software. Because the intensity of illumination by the mercury lamp varies from time to time, and because the amount of time for image acquisition was adjusted for each experiment so that the gain was within the limits of the linear response range, it is not possible to compare absolute fluorescence intensities measured for different experiments. Cells were flattened onto the coverslip during the mounting process, and only the fluorescence intensity from the brightest focal plane was measured. Cells were first chosen at random in the phase channel and were then checked for nuclear morphology by 4',6'-diamidino-2-phenylidole (DAPI) staining (Sigma). Cells that had lost the refractile appearance or the nucleus (only ~5–10% of total population) were not considered further. For each data set, 30–50 cells from five different fields that were chosen at random were measured. An area from each field that did not have cells was also measured as the background reading that was subtracted from the measured fluorescence intensity of the cells in the corresponding field. Because actin incorporation occurs asynchronously across the cell population, we assessed the kinetics of actin polymerization by taking the average of the highest 20% of fluorescence measurements for each time point. These kinetics, therefore, compare the cell populations that assemble actin most efficiently. All of the experiments in this paper have been repeated at least three times. Although absolute fluorescence intensities measured were not always identical each time the experiment was repeated, the data obtained from the different trials were all qualitatively similar.

Results

A Yeast Permeabilized Cell Assay for Polarized Actin Assembly

Three obstacles had to be overcome to develop a permeabilized cell assay for polarized actin assembly in yeast. First, detergent treatment alone does not permeabilize yeast cells because of the presence of the cell wall. Second, enzymatic removal of the cell wall causes actin redistribution and loss of cell polarity and, therefore, is not desirable. Third, yeast actin rearranges rapidly (within minutes) in response to changes in environmental factors such as osmolarity, pH, and temperature (Chowdhury et al., 1992; Drubin, D., unpublished results). To circumvent these problems, we took advantage of an observation made by electron microscopy (McDonald, K., personal communication) that freezing yeast cells in liquid nitrogen introduces small discontinuities in the cell wall. Furthermore, quick freezing in the absence of glycerol kills essentially 100% of the cells (data not shown) and, therefore, may eliminate the problem of cytoskeletal rearrangement during cell permeabilization. Thus, cells were frozen in liquid nitrogen, thawed, and then treated with saponin, a cholesterol-chelating detergent, to permeabilize the plasma membrane. 70 kD fluorescein-labeled dextran can enter ≥60% of the cells from an exponentially growing culture permeabilized by this procedure. Both the quick freeze and the detergent treatment steps are essential for efficient permeabilization.

We determined whether cells thus permeabilized have the ability to incorporate exogenously added actin in a pattern similar to the actin distribution in living cells. After saponin treatment, rhodamine-labeled actin (Rd-actin) monomers were added to the cells in a buffer that promotes actin assembly. After 10 min, the cells were fixed and 70 kD fluorescein-labeled dextran was added to identify the permeabilized cells. Among the permeabilized cells with small buds, (smaller than one third the size of the mother), ~80% incorporate Rd-actin into the bud (Fig. 1, *C* and *D*). Cells that are not permeabilized do not incorporate any rhodamine actin. We compared the pattern of actin assembly in permeabilized cells prepared at various cell cycle stages with the in vivo cortical actin distribution at the corresponding cell cycles stages (Fig. 2). Cells that are treated with a low level of α factor arrest in G1, but they do not form mating projections (Reed et al., 1992). These cells display an isotropic cortical actin distribution (Fig. 2 *B*, *a*). Permeabilized G1 cells exhibit a low level of nucleation activity that is randomly distributed (Fig. 2 *A*, *a*). Upon removal of the α factor, cells

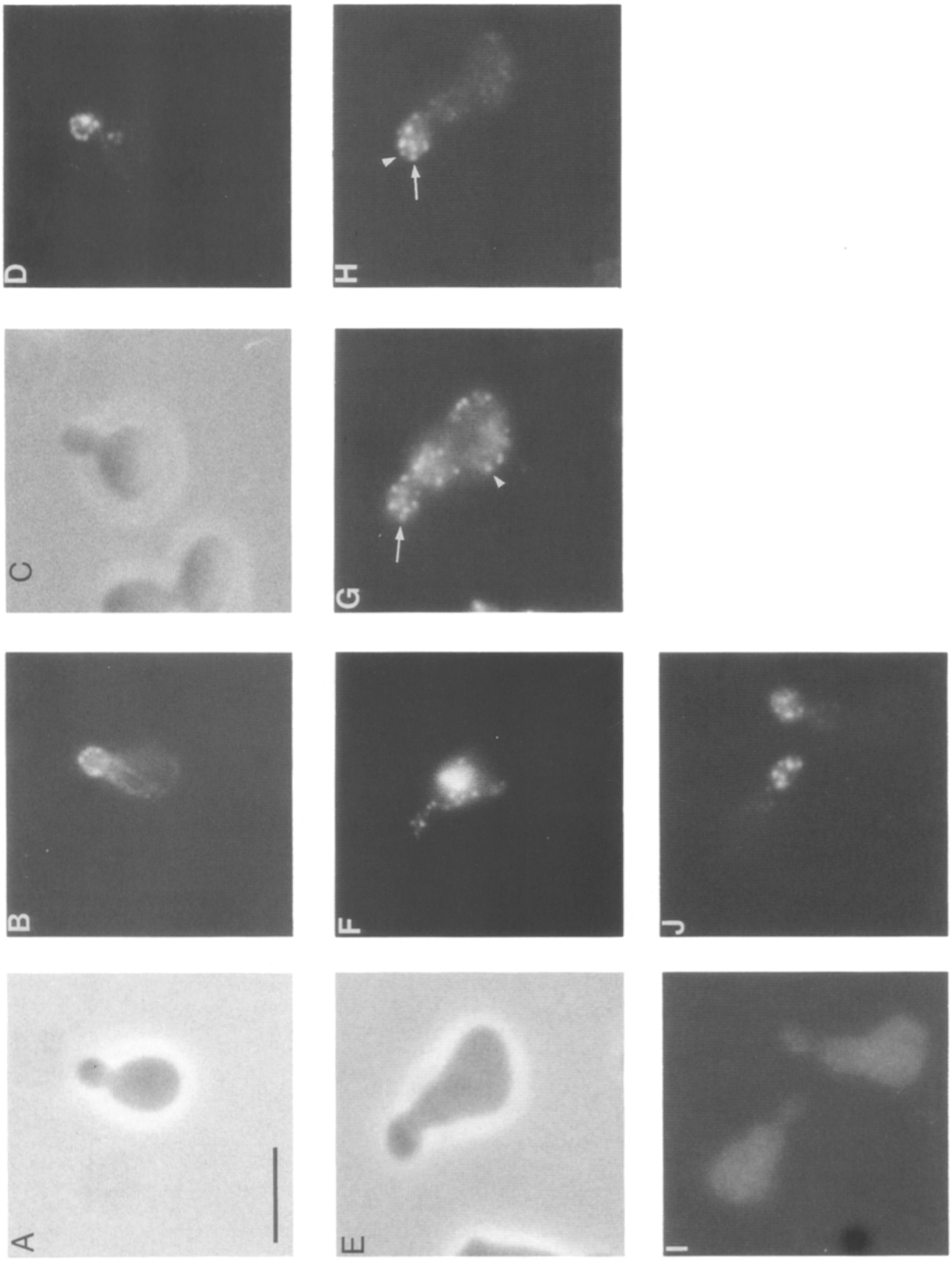
D
H
C
G
B
F
J
A
E
I

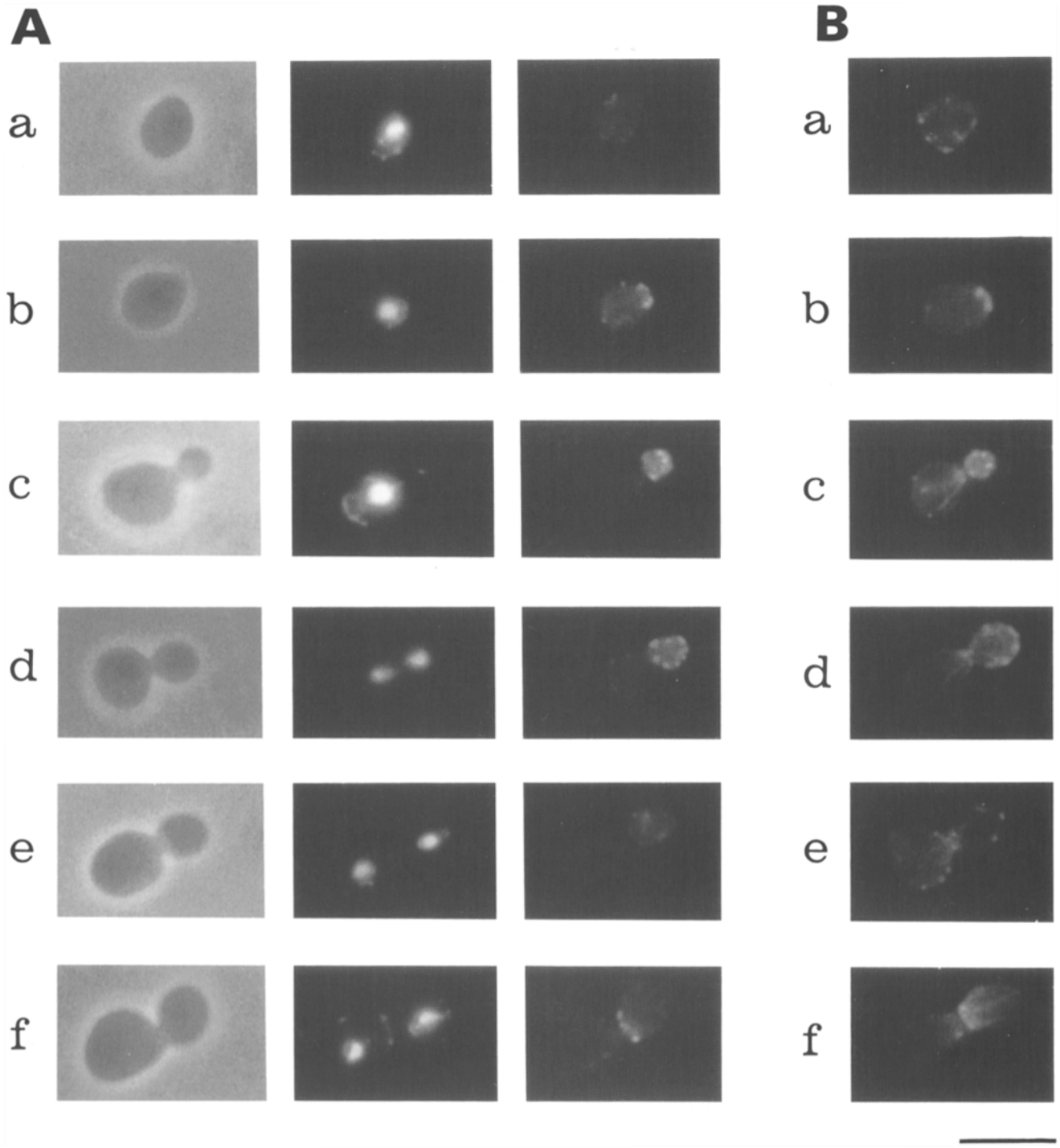

Figure 2. Cell cycle dependence of the pattern of actin assembly in permeabilized yeast cells. A mid-log phase culture was treated with 0.1 μg/ml α factor for 1 h at 30°C. The cells were washed, resuspended in YPD, and grown at 30°C. At 0, 30, 40, 50, 60, and 70 min after α factor removal, one aliquot of the cells was frozen, permeabilized, and assayed for Rd-actin incorporation (*A*). Phase (*left panels*), DAPI (*middle panels*), and rhodamine fluorescence (*right panels*) images of cells are shown. (*a–f*) represent successive cell cycle stages as indicated by the bud and nuclear morphologies. In parallel at each time point, an aliquot of the cells was fixed directly with formaldehyde in the growth media, and the cells were stained with fluorescein-phalloidin (*B*). Fluorescein fluorescence images of cells at the same cell cycle stages as the cells shown on the left in (*A*) are shown. Bar, 10 μm.

Figure 1. Permeabilized yeast cells incorporate exogenous actin into cortical patches in the bud. Phase (*A*) and fluorescein fluorescence image (*B*) of a cell from an exponentially growing culture that was fixed and stained with fluorescein-phalloidin. Phase (*C*) and rhodamine fluorescence image (*D*) of a cell from the same culture as *A* that was permeabilized and incorporated Rd-actin for 8 min under the conditions described in Materials and Methods. Phase image (*E*), DAPI staining of nuclear and mitochondrial DNA (*F*), actin immunofluorescence (*G*), and Rd-actin fluorescence (*H*) of a cell from a culture enriched for the small-budded cells after Rd-actin incorporation. Arrows in *G* and *H* point to an actin patch that contains both the endogenous actin and the incorporated Rd-actin. Arrowheads in *G* and *H* point to actin patches that contain either the endogenous actin or the incorporated Rd-actin, but not both. Incorporation of a 70-kD fluorescein-dextran into permeabilized cells (*I*) (see Materials and Methods) and Rd-actin assembly in the same cells (*J*). Bar, 10 μm.

were synchronously released from the G1 arrest and ~30 min later, a ring of cortical actin appears at the presumptive bud site (Fig. 2 *B*, *b*). Rd-actin patches formed in vitro in permeabilized cells prepared from this stage show the same distribution (Fig. 2 *A*, *b*). Throughout bud growth and until sometime after nuclear division, cortical actin patches formed in vivo and in vitro are seen predominantly in the bud (Fig. 2, *A*, *c* and *d*, and *B*, *c* and *d*). After nuclear division, cortical actin patches become evenly distributed in the bud and the mother, and the cells grow isotropically (Fig. 2 *B*, *e*). Cells permeabilized at this stage exhibit a low nucleation activity in the bud which is as low as that in the mother (Fig. 2 *A*, *e*). Finally, at cytokinesis, cortical actin is concentrated at the septum (Fig. 2 *B*, *f*), and this pattern is reflected in the Rd-actin assembly pattern in the permeabilized cells (Fig. 2 *A*, *f*). These results demonstrate that the spatial organization of the nucleation sites observed in the permeabilized cells is subjected to cell cycle control, and that the in vitro actin assembly pattern reflects the in vivo actin distribution during apical growth and cytokinesis.

Because small-budded cells have the advantages of having a highly characteristic pattern of actin organization that is readily assessed (patches are concentrated in the bud), and they are rapidly forming new actin patches at the time the cell is frozen since the surface area of small buds is rapidly expanding, for all subsequent experiments, we enriched for the small-budded cell population by freezing cells ~45 min after release from an α factor arrest. Greater than 80% of the cells thus prepared were small-budded cells with undivided nuclei. Another advantage of using the small-budded cells enriched by this procedure is that these cells are permeabilized more efficiently (>85%) than cells from an asynchronous culture. Since the pattern of actin incorporation into these cells (Fig. 1, *H* and *J*) is similar to the pattern for small-budded cells from an asynchronous culture (Fig. 1 *D*), this method of enriching for the small-budded cells was used in most of the subsequent experiments. Exogenously added Rd-actin assembles into dotlike structures of similar appearance to endogenous actin patches (Fig. 1). When the permeabilized cells were stained with an antibody that recognizes only yeast actin but not rabbit muscle actin (Drubin et al., 1988), in some but, significantly, not in all cases (see Discussion), the Rd-actin fluorescence coincides with preexisting actin patches (Fig. 1, *G* and *H*). The mothers of the permeabilized cells seem to have gained some actin structures that may consist of cytoplasmic cables that have collapsed during freezing and thawing (Fig. 1 *G*), but these patches do not incorporate Rd-actin (Fig. 1 *H*). Actin cables, however, do not form in the permeabilized cells, possibly because of the absence of cytosolic factors. Because fluorescein dextran added to the permeabilized cells is evenly distributed throughout the cells, it is unlikely that the preferential incorporation of actin into the bud is caused by differences between the access of monomers to the bud versus the mother cell (Fig. 1, *I* and *J*).

The level of Rd-actin assembly in the permeabilized cells can be quantified by displaying the fluorescent images on a computer screen and measuring the average fluorescence intensity in specific regions of the cell, i.e., the bud or the mother (see Materials and Methods). Four lines of evidence indicate that Rd-actin incorporation into the bud of permeabilized yeast cells comes from actin polymerization. First, since ADP-bound actin polymerizes much more slowly and only at a much higher concentration than the ATP-bound form (Pollard, 1984, 1986), we prepared ADP-actin and examined its incorporation in the permeabilized cells. The level of ADP-actin incorporation is less than one tenth that of ATP-actin (Table II). Second, if salt is left out of the polymerization buffer, a condition that is unfavorable for polymerization, incorporation of Rd-actin into the permeabilized cells does not occur (Table II). Third, actin incorporation into the bud is significantly reduced if 40 nM cytochalasin D (CD), a drug that binds to the barbed ends of actin filaments blocking polymerization (Brown and Spudich, 1981), is present during the Rd-actin incorporation step (Table II). Finally, the incorporated rhodamine fluorescence (Fig. 3 *A*) disappears from the bud upon dilution of the monomer pool (Fig. 3 *B*), but the fluorescence loss can be prevented if phalloidin, a drug that is known to stabilize actin polymer (Estes et al., 1981), is included in the dilution buffer (Fig. 3 *C*). These results, taken together, strongly suggest that the accumulation of rhodamine fluorescence in the bud requires actin polymerization.

An Actin Nucleation Activity Is Required for Actin Assembly in the Bud of Permeabilized Cells

The kinetics of actin incorporation into the permeabilized cells at 0.5 μM Rd-actin concentration were determined by fixing cells at different time points after Rd-actin addition and measuring the fluorescence intensity in the bud or the mother at each time point as described in Materials and Methods. Fig. 4 *A* shows the levels of rhodamine fluorescence in the bud for the entire cell population at each time point. Because, at a given time point, cells incorporate exogenous actin at different rates, a fact that may result from differences in cell physiology, preservation of cellular structures during the permeabilization step, and/or differences in cell permeability, we assessed the kinetics of actin polymerization by considering the fastest actin-incorporating cell population (Fig. 4 *B*; see Materials and Methods). The average of the fluorescence incorporated in this population was

Table II. Conditions and Treatments That Affect Actin Incorporation into Permeabilized Yeast Cells

Condition	Actin incorporation
ADP-actin	–
Filamentous actin	–
G buffer	–
40 nM cytochalasin D	–*
0.5 M KCl	–
0.1% Triton X-100	+
Trypsin	–

Treatments with KCl and Triton X-100 were carried out as follows: cells were incubated with U buffer containing 0.5 M KCl or 0.1% Triton X-100 for 20 min at 25°C, then washed with U buffer alone before initiation of the actin assembly reaction. Trypsin treatment was carried out as described in Materials and Methods. –, Rd-actin incorporation in the treated cells or under the specified conditions is <10% of that in the control; +, Rd-actin incorporation is ≥80% of that in the control. * The presence of 40 nM CD during the assembly reaction only reduces Rd-actin incorporation by ~60%, but this level of inhibition is comparable to that observed on pyrene actin assembly in solution (data not shown). The controls are: ATP-actin for ADP-actin, G-actin for F-actin, U buffer (Materials and Methods) for KCl and Triton X-100, U buffer + ATP for G buffer (Materials and Methods) and U buffer + ATP + CD, and U buffer + trypsin + trypsin inhibitor for trypsin treatment.

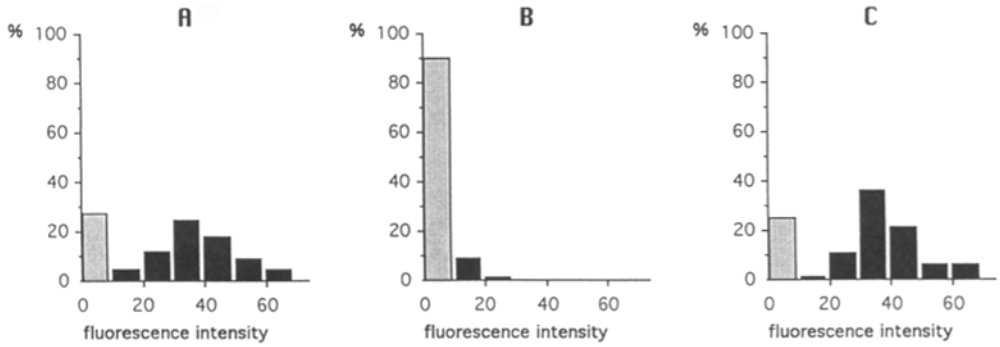

Figure 3. Rd-actin incorporation into permeabilized cells results from actin polymerization. 0.5 μM Rd-actin was added to permeabilized small-budded cells in polymerization buffer, and the reaction was terminated after incubation at 25°C for 8 min (*A*). Alternatively, after incubation at 25°C for 8 min, cells were pelleted, the supernatant was removed, and the cell pellet was immediately resuspended in 100 μl polymerization buffer without Rd-actin (*B*) or in polymerization buffer containing 5 μM phalloidin without Rd-actin (*C*). Formaldehyde was added to 5% after incubation at 25°C for 20 min. The intensity of the incorporated rhodamine fluorescence in the bud and the mother was quantified (see Materials and Methods). The graphs show the distribution of the incorporated levels of rhodamine fluorescence in the bud across the cell population. The stippled bars represent the population of cells whose buds have the same background level of fluorescence as the mother cell. The units of fluorescence intensity are arbitrary.

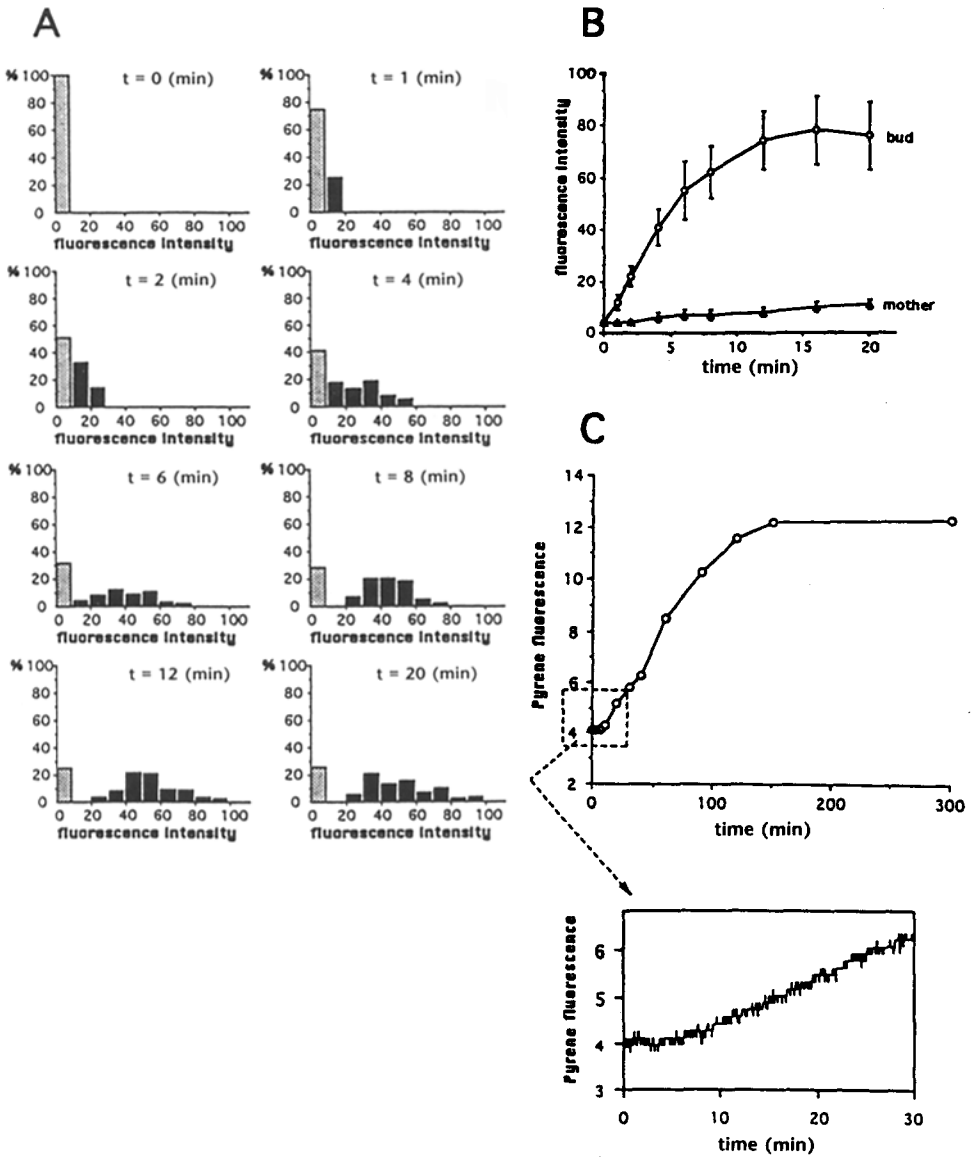

Figure 4. Kinetics of actin polymerization in permeabilized yeast cells. 0.5 μM Rd-actin was added to permeabilized small-budded cells in polymerization buffer. Aliquots of the cells were fixed at different times at 25°C. The intensity of the incorporated rhodamine fluorescence in the bud and the mother was quantified (see Materials and Methods). (*A*) The distribution of the incorporated levels of rhodamine fluorescence in the bud across the entire cell population at each time point. The stippled bars represent the population of cells whose buds have the same background level of fluorescence as the mother cell. (*B*) A plot of the average fluorescence intensity taken from the highest 20% fluorescence measurements from each time point over time. (*C*) Spontaneous actin polymerization at 0.5 μM determined by the pyrene-actin coassembly assay (see Materials and Methods). The units of fluorescence intensity are arbitrary.

plotted over time. Rd-actin polymerization in the bud does not have a lag phase (Fig. 4 *B*). Polymerization proceeds linearly during the first 6–8 min and reaches saturation after ~12 min. Because polymerization of 0.5 μM actin in solution displays an 8–10-min lag phase (Fig. 4 *C*), corresponding to the nucleation step for spontaneous filament assembly (Pollard and Craig, 1982), there must be an activity present in the bud of the permeabilized cells that facilitates the nucleation step of actin polymerization.

Rd-actin polymerization in the bud appears to be saturable (Fig. 4, *A* and *B*). This saturation might be caused by the depletion of the monomer pool by spontaneous filament formation outside the cells, or alternatively, it might be caused by intrinsic properties of the cell cortex. To distinguish between these two possibilities, a Rd-actin polymerization reaction was first initiated in the absence of the cells. At various times, the polymerization reaction was added to the permeabilized cells and was incubated with the cells for 8 min. Fig. 5 *A* shows that polymerization for ≤40 min before incubation with the cells, a time at which ~25% of total spontaneous polymerization has occurred (estimated from Fig. 4 *C*), has little effect on the amount of actin incorporated into the buds. To directly demonstrate that the extent of filament assembly is restricted by the cell cortex, unlabeled actin was first allowed to polymerize in the permeabilized cells for various amounts of time and was then replaced with the same concentration of Rd-actin in polymerization buffer for 8 min. The amount of Rd-actin incorporated in the bud is reduced as the time of previous polymerization with unlabeled actin is increased (Fig. 5 *B*).

Actin Polymerization in Permeabilized Yeast Cells Is Nucleated by Protein Factors Distinct from the Barbed Ends of Actin Filaments

Because the lack of a lag phase for actin polymerization in the bud implies the presence of an actin nucleation activity, we set out to determine the biochemical nature of this activity. Treatment of the permeabilized cells with trypsin or 0.5 M KCl before Rd-actin addition abolishes Rd-actin incorporation, indicating that protein factors are required for nucleating actin assembly (Table II). Furthermore, treating cells with trypsin before detergent treatment also eliminates actin incorporation (Fig. 6 *A*, *a* and *b*), and under these conditions, endogenous actin does not appear to have been proteolyzed (Fig. 6 *B*, lanes *1* and *2*). (Endogenous actin can be proteolyzed if trypsin is added after detergent treatment [Fig. 6 *B*, lanes *3* and *4*]). These results suggest that the endogenous actin alone is not sufficient for nucleating actin assembly.

Three lines of evidence suggest that the ends of endogenous actin filaments are not responsible for actin nucleation in permeabilized yeast cells. First, to test the possibility that actin assembly is nucleated from the barbed ends (fast-growing ends) of existing filaments, we determined whether the nucleation activity is inhibited by CD treatment. To establish conditions for this experiment, stabilized yeast actin filaments were incubated with 200 nM CD for 20 min. An aliquot of the reaction was diluted 100-fold into a pyrene actin assembly reaction (see Materials and Methods). The rate constant for CD dissociation from the barbed ends has not been reported in the literature. By measuring the initial rate of pyrene actin polymerization at various times after dilution

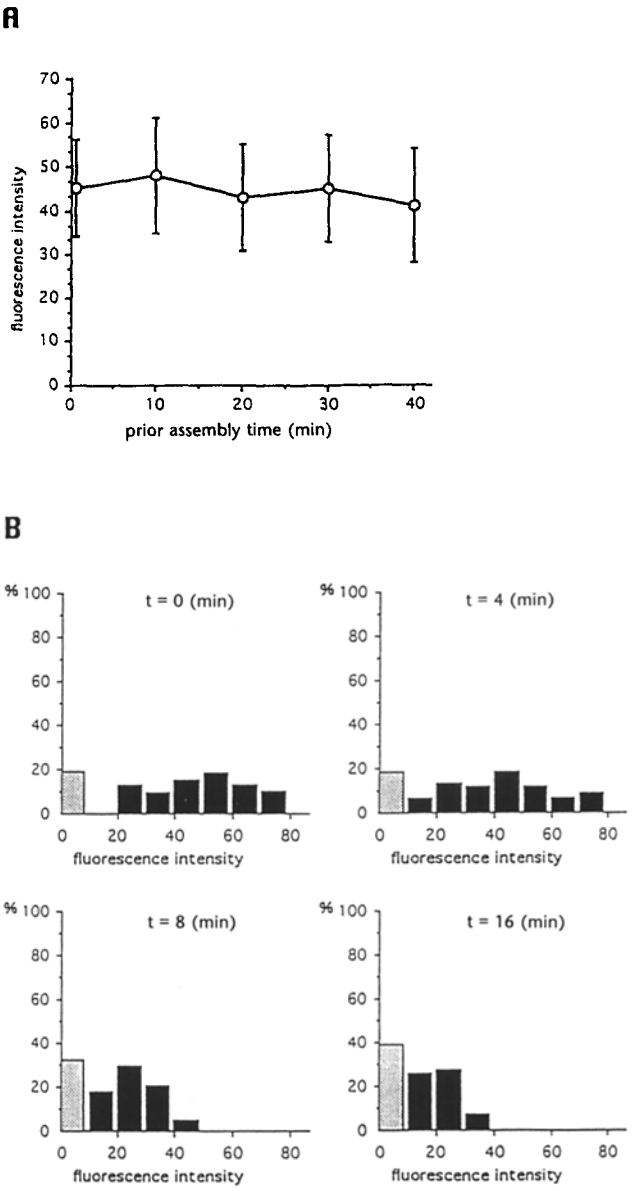

Figure 5. Rd-actin assembly in the bud is saturable. (*A*) Rd-actin polymerization reactions at 0.5 μM monomer concentration were first initiated in the absence of the cells in U buffer containing 1 mM ATP, and they were added to the permeabilized small-budded cells at various times, as indicated by the horizontal scale. Cells were fixed with formaldehyde after 8 min to stop actin assembly. The intensity of the incorporated rhodamine fluorescence in the bud was quantified as shown. (*B*) 0.5 μM unlabeled actin was first allowed to polymerize in the permeabilized small-budded cells for various amounts of time as indicated above each histogram. Cells were pelleted, and 20 μl of Rd-actin in U buffer containing 1 mM ATP was added to the cells. The reactions were stopped after 8 min. The stippled bars represent the population of cells whose buds have the same background level of fluorescence as the mother cell.

of the capping reaction, we estimated that under the conditions described above, the half-life of CD-capped ends is ~4 min (data not shown). As shown in Fig. 7 *A*, yeast F-actin stimulates pyrene actin polymerization by providing nucleation sites, but the stimulatory effect is reduced by 73% (comparing pyrene fluorescence levels at 4 min) if the F-actin has

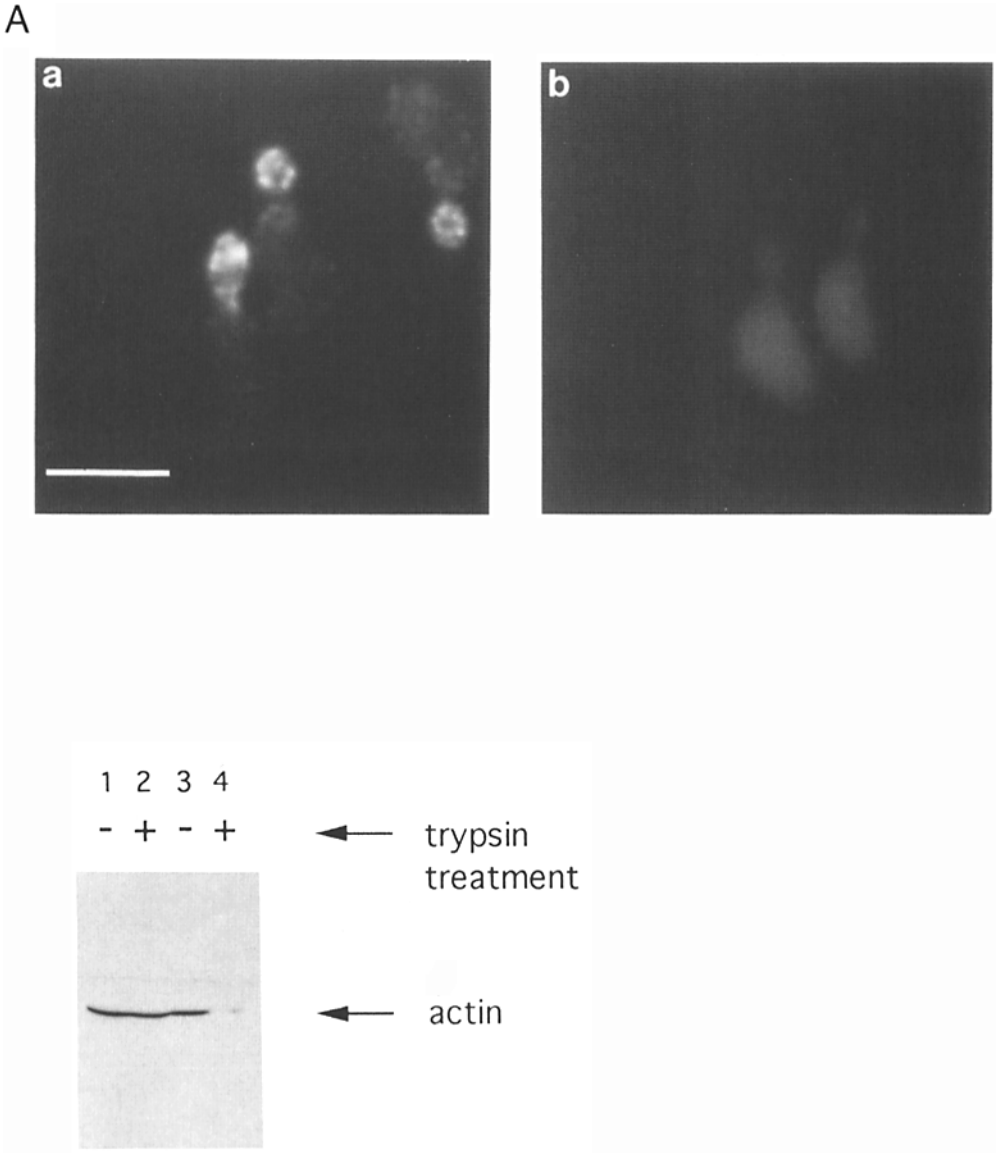

Figure 6. Actin nucleation in permeabilized yeast cells is sensitive to external trypsin treatment. (*A*) Frozen SB cells were thawed. Treatment of nonpermeabilized cells with a control reaction lacking trypsin (*a*) or with 50 μg/ml trypsin (*b*) was carried out as described in Materials and Methods. The cells were then washed with buffer and Rd-actin assembly was carried out as described in the legend of Fig. 3 *A*. Rhodamine fluorescence images of cells representative of each treatment are shown. Bar, 10 μm. (*B*) Immunoblot analysis of extracts from control cells and trypsin-treated cells using rabbit antiactin primary antibody and the ECL detection method (see Materials and Methods). Trypsin treatment was carried out either before (lanes *1* and *2*) or after (lanes *3* and *4*) membrane permeabilization by saponin. Lanes *1* and *3* contain extracts from cells that were not treated with trypsin.

been incubated with 200 nM CD before monomer addition. Since 2 nM CD (the CD concentration after 100-fold dilution) has no detectable effect on polymerization (data not shown), the reduced rate and extent of pyrene fluorescence increase is likely to be caused by capping of the barbed ends of yeast actin filaments during the incubation with 200 nM CD. Next, we treated the permeabilized cells with 200 nM CD and then carried out Rd-actin polymerization reactions in the presence of 2 nM CD. Treatment with 200 nM CD before monomer addition did not reduce the level of actin incorporation into the bud (Fig. 7 *B*). The same result was obtained when higher concentrations of CD (≤20 μM) were used during the treatment before monomer addition (data not shown). Second, because the concentration of Rd-actin used in the assay is lower than or similar to the critical concentration for pointed-end assembly (Pollard and Cooper, 1986), the pointed ends of the endogenous filaments should not contribute significantly to the nucleation activity, unless an additional activity that facilitates pointed end elongation is also present. Third, the nucleation activity is completely abolished by an external protease treatment that does not degrade the endogenous actin (Fig. 6 *A*). Furthermore, the difference in Rd-actin incorporation in the bud and the mother can not be accounted for simply by the difference in the amount of endogenous actin filaments preserved in these two parts of the permeabilized cells (Fig. 1, *G* and *H*). These results suggest that actin polymerization in permeabilized yeast cells is nucleated by protein factors distinct from ends of actin filaments.

The Kinetics of Actin Assembly Is Altered in Capping Protein Mutants

A possible explanation for why new filament polymerization can not be nucleated from endogenous filaments is that the barbed ends of these filaments are blocked by capping proteins. A yeast capping protein homologous to the capping protein identified in many other eukaryotic cells is a heterodimer encoded by the *CAP1* and *CAP2* genes (Amatruda et al., 1990, 1992*b*). Disruption of *CAP2* is not lethal, but it

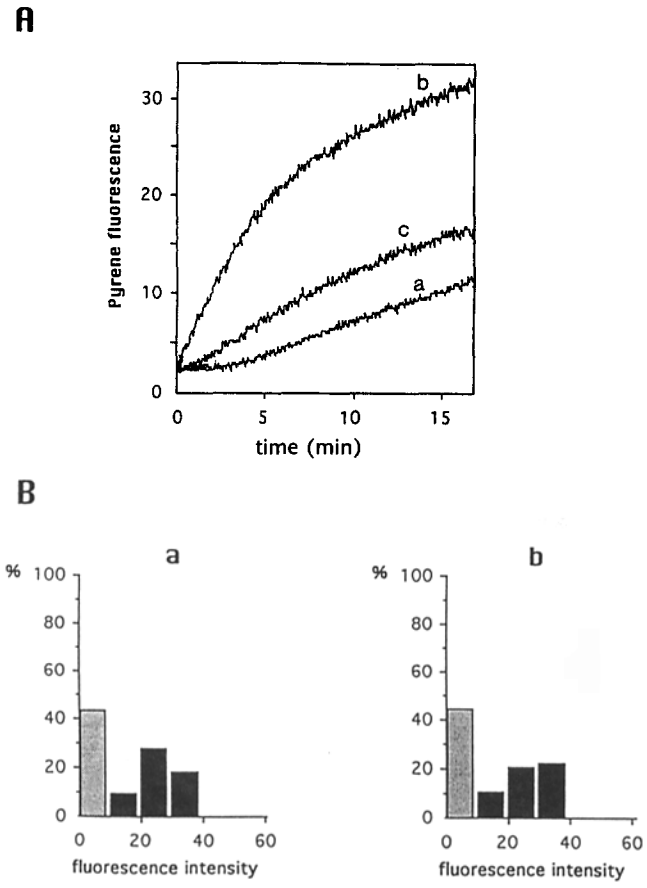

Figure 7. Cytochalasin D does not inhibit the actin nucleation activity in the bud. (*A*) F-actin was prepared by polymerizing 5 μM yeast actin for 30 min in U buffer containing 1 mM ATP. 5 μM phalloidin was added to the polymerization reaction and incubated further for ≥30 min. For CD treatment, yeast F-actin was incubated with 200 nM CD for 30 min at 25°C. Assembly of 1 μM rabbit muscle actin (20% pyrene-labeled) was carried out in the absence of yeast F-actin (*a*), in the presence of 0.05 μM yeast F-actin (*b*), or in the presence of 0.05 μM yeast F-actin that has been incubated with CD for 30 min (*c*). The final CD concentration during the pyrene-actin assembly reaction in *c* was 2 nM resulting from a 1-100 dilution of (F-actin + 200 nM CD) into the assembly reaction. The unit of fluorescence intensity is arbitrary. (*B*) Permeabilized small-budded cells were incubated with (*b*) or without (*a*) 200 nM CD in U buffer for 20 min at 25°C. Cells were pelleted, rapidly washed one time with polymerization buffer containing 2 nM CD, and were incubated with 0.5 μM Rd-actin in polymerization buffer containing 2 nM CD for 4 min before they were fixed with formaldehyde. The distributions of incorporated levels of rhodamine fluorescence in the bud across the cell population are shown. The stippled bars represent the population of cells whose buds have the same background level of fluorescence as the mother cell. The unit of fluorescence intensity is arbitrary.

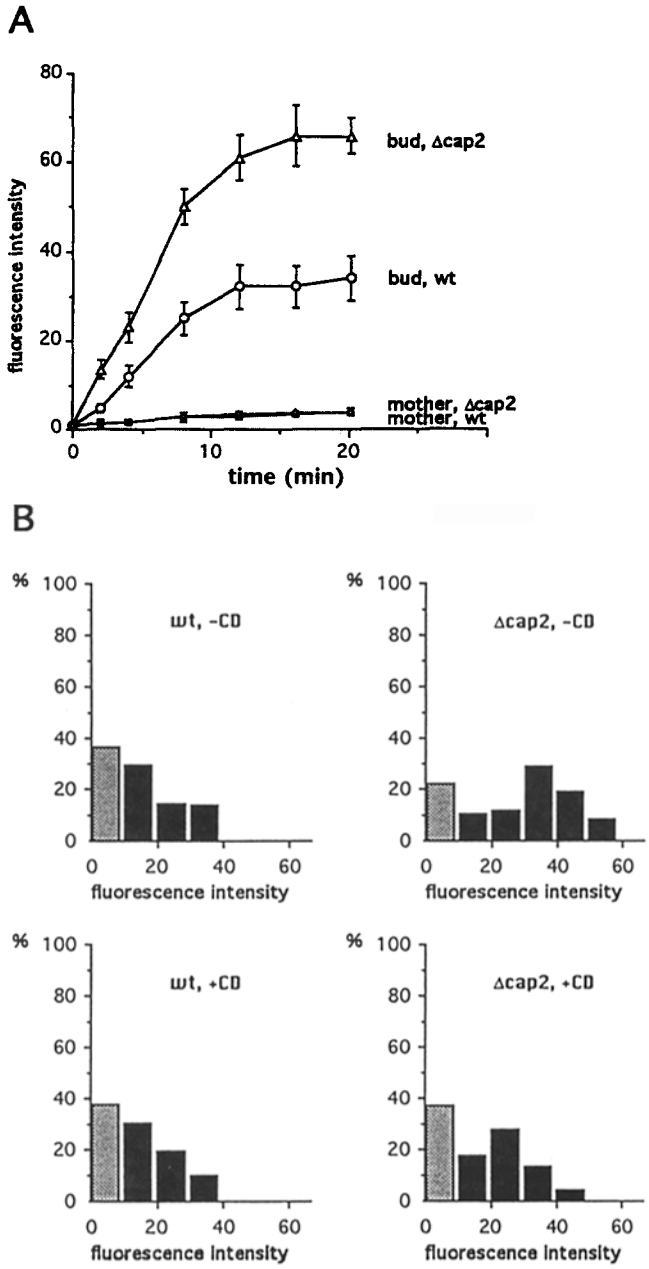

Figure 8. The kinetics and the saturation level of actin assembly are altered in capping protein mutants. (*A*) 0.5 μM Rd-actin was added to permeabilized wild-type (JC93) and Δ*cap2* (JC108) small-budded cells in polymerization buffer. Aliquots of the cells were fixed at different times at 25°C. The intensity of the incorporated rhodamine fluorescence in the bud and the mother was quantified. The average taken from the highest 20% fluorescence measurements from each time point was plotted over time. (*B*) Permeabilized wild-type and Δ*cap* SB cells were subjected to the same treatment as described in the legend of Fig. 7 *B*. The intensity of the incorporated rhodamine fluorescence in the bud was quantified as shown. The unit of fluorescence intensity is arbitrary.

causes morphological abnormalities during bud growth (Amatruda et al., 1990). We tested whether permeabilized Δ*cap2* cells show a difference in actin assembly compared to permeabilized wild-type cells. Wild-type and Δ*cap2* cells were permeabilized to a similar extent as judged by fluorescein dextran incorporation (data not shown). Fig. 8 *A* shows that the rate of actin assembly is significantly increased in Δ*cap2* cells, suggesting that Δ*cap2* cells contain more nucleation sites than wild-type cells as a result of uncapping of barbed ends. This possibility is further supported by the result that treating permeabilized Δ*cap2* cells with CD before the assembly reaction reduces actin incorporation within the initial 4-min period, which reflects the rate of actin assem-

bly, to a level similar to that observed in wild-type cells pretreated or not pretreated with CD (Fig. 8 *B*). Significantly, the level of actin assembly saturation is also much higher in the buds of Δ*cap2* cells than in the buds of wild-type cells (Fig. 8 *A*), and the Δ*cap2* mutation does not increase the level of Rd-actin incorporation in the mother cells (Fig. 8 *A*).

The Involvement of Actin Cytoskeletal Components in Nucleating Actin Assembly

To test the importance of previously identified cytoskeletal components in actin nucleation, we performed the in vitro actin assembly assay on mutants that contain null alleles of genes that encode components of the actin cytoskeleton. Wild-type and mutant cells enriched for the population that have small buds and undivided nuclei were permeabilized. As shown in Fig. 9, *A* and *B*, permeabilized small-budded cells that lack *ABP1* or *SAC6*, encoding a filament binding protein and a filament bundling protein, respectively (Drubin et al., 1988; Adams et al., 1989), show similar levels of actin incorporation to that in wild-type cells. Rd-actin incorporation in the buds of Δ*sla1* and Δ*sla2* cells grown at the permissive temperature (25°C), on the other hand, is reduced to <10% of that in wild-type cells (Fig. 9, *C* and *D*). The defects in actin incorporation in Δ*sla1* and Δ*sla2* cells is not caused by the lack of permeability because the cells can incorporate the 70-kD fluorescein dextran to the same extent as wild-type cells (data not shown). It is possible that Sla1 (an SH3 domain-containing protein) and Sla2 (a protein with sequence homology to talin) are components of the actin nucleation sites.

GTP-γS Stimulates Actin Assembly in Permeabilized Cells

GTP-binding proteins have been implicated in the regulation of actin cytoskeletal changes during cellular morphogenesis (reviewed in Hall et al., 1992). In yeast, mutations that impair the function of Cdc42, a Rho-like GTP-binding protein, abolish polarized growth and polarized cytoskeleton assembly (Johnson and Pringle, 1990). To investigate the relationship between GTP-binding protein activation and polarized actin cytoskeleton assembly, we first examined the effect of GTP-γS, a poorly hydrolyzable GTP analogue, on the actin nucleation activity in permeabilized cells. After detergent permeabilization, cells were incubated with 0.2 mM GTP-γS, then washed with the buffer, and actin polymerization was carried out. When the polymerization reaction was terminated at 4 min, a time that falls within the linear phase of polymerization both in the absence (Fig. 4 *B*) and in the presence (not shown) of GTP-γS, cells that have been treated with GTP-γS show a significant increase (about twofold on average) in Rd-actin incorporation in the bud compared to the untreated cells (Fig. 10, *A* and *B*). Cells treated with 0.2 mM ATP-γS (an ATP analogue) or 0.2 mM GDP-βS (a GDP analogue that is not readily converted to GTP) do not show a stimulated level of actin incorporation (data not shown). When the polymerization reaction was allowed to reach saturation, a difference in Rd-actin incorporation in GTP-γS-treated and -untreated cells is not apparent (Fig. 10, *C* and *D*). The above results suggest that GTP-γS affects the kinetics, but not the saturation level, of the assembly reaction.

A Mutation in CDC42 Abolishes Actin Polymerization in the Bud

A temperature-sensitive *cdc42* mutant, *cdc42-1*, was used to determine whether Cdc42p mediates the GTP-γS effect. To separate the cell cycle–regulated changes in actin distribution from those resulting directly from the temperature-sensitive mutation, we used hydroxyurea, a DNA synthesis inhibitor, to block cell cycle progression in S-phase and, therefore, maintain a population undergoing apical growth (Sloat et al., 1981). When *cdc42-1* cells are released from the α factor arrest to growth in the presence of 10 mg/ml hydroxyurea at 28°C, a semipermissive temperature, bud emergence occurs in ~75% of the cells, but it takes a longer time than in wild-type cells (60 min instead of 45 min). The *cdc42-1* cells grown at 28°C are rounder than wild-type cells, suggesting that apical growth and, therefore, Cdc42p function are partially compromised at this temperature. These cells show a significant decrease in Rd-actin incorporation compared to wild-type cells (compare Fig. 10, *E* versus *A*). This defect in actin incorporation in *cdc42-1* cells is not caused by a reduction in permeability because the cells can incorporate the 70-kD fluorescein dextran to the same extent as wild-type cells (data not shown). Furthermore, actin polymerization in *cdc42-1* cells grown at 28°C can not be stimulated by preincubating the cells with GTP-γS (compare Fig. 10, *E* versus *F*). When the budded *cdc42-1* cells were shifted to 37°C, the nonpermissive temperature, for 40 min in the presence of 10 mg/ml hydroxyurea, only 12% of the permeabilized *cdc42-1* cells were able to nucleate actin assembly (compared to 80% of the wild-type population), and the level of actin incorporation in these cells is reduced to <10% of that in wild-type cells (data not shown). These results show that *CDC42* function is required for actin assembly in the bud.

The Loss of Actin Nucleation Activity in cdc42-1 Mutant Cells Can Be Complemented In Vitro by a Constitutively Active Cdc42 Protein

To test the possibility that Cdc42p plays a direct role in regulating actin assembly, we determined whether the loss of actin nucleation activity in *cdc42-1* mutant can be complemented in vitro by purified Cdc42 proteins. Because wild-type Cdc42 protein rapidly hydrolyzes the bound GTP and thus exists largely in its inactive GDP-bound form (Zheng et al., 1994), we used the constitutively active $Cdc42^{L61}$ mutant protein for these experiments (Ziman et al., 1991). *cdc42-1* cells grown at 28°C were permeabilized and then incubated with purified $Cdc42^{L61}$ protein bound with GTP, or with wild-type Cdc42p bound with GDP, for 30 min at 30°C. The cells were washed with polymerization buffer before initiation of the Rd-actin assembly reaction. Only 30% of the budded *cdc42-1* cells that have been incubated with the control buffer incorporate Rd-actin (Fig. 11 *D*). After incubation with $Cdc42^{L61}$ mutant protein, the percent of the budded *cdc42-1* cells that incorporate Rd-actin is increased to 75% (Fig. 11 *F*), almost as high as that observed among the wild-type cell population (Fig. 11 *A*). As shown in Fig. 11 *H*, actin incorporation in *cdc42-1* cells incubated with $Cdc42^{L61}$p is spatially restricted to the bud. *cdc42-1* cells incubated with the GDP-bound Cdc42 protein, on the other hand, only demonstrate a slight improvement in Rd-actin polymerization

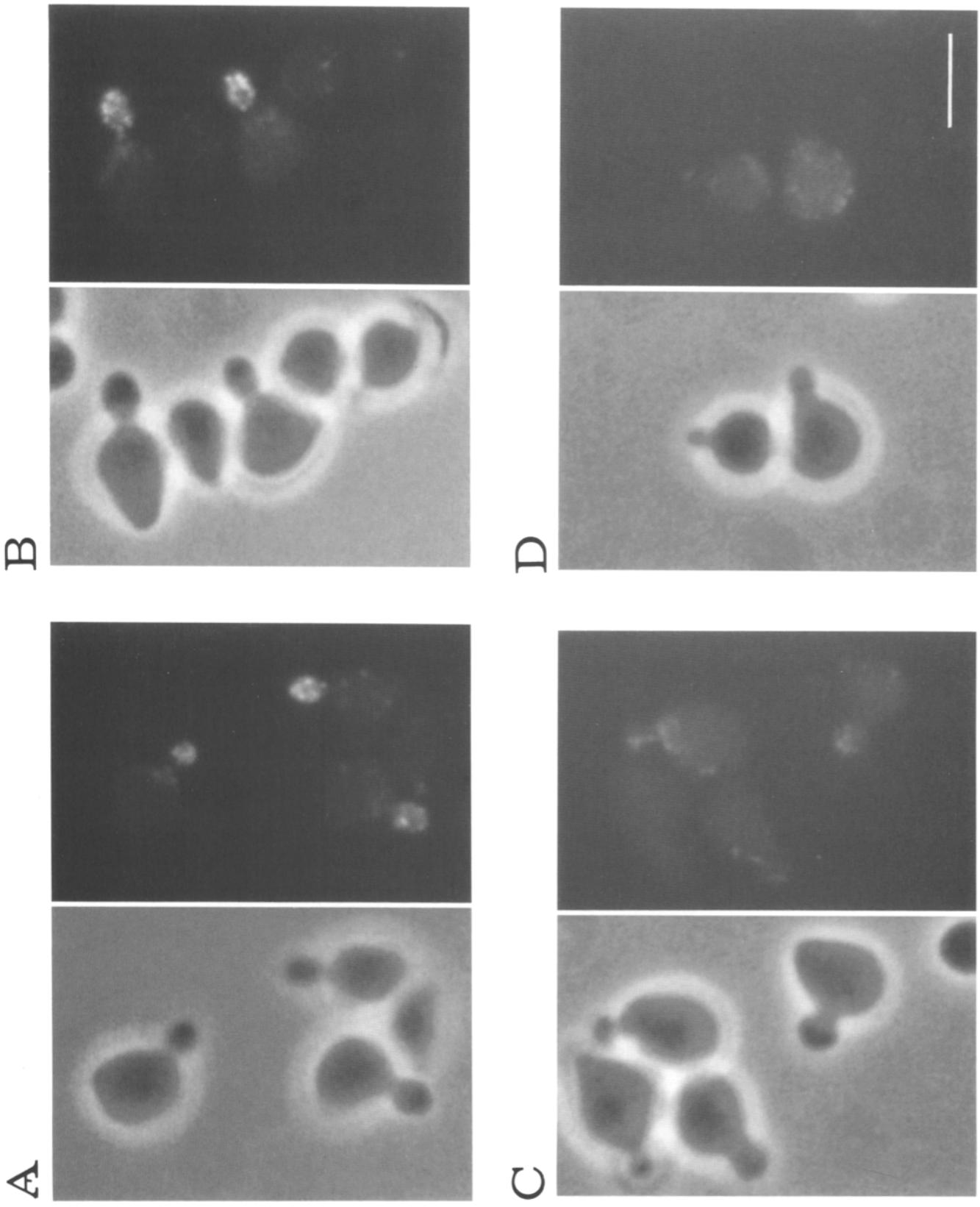
A
B
C
D

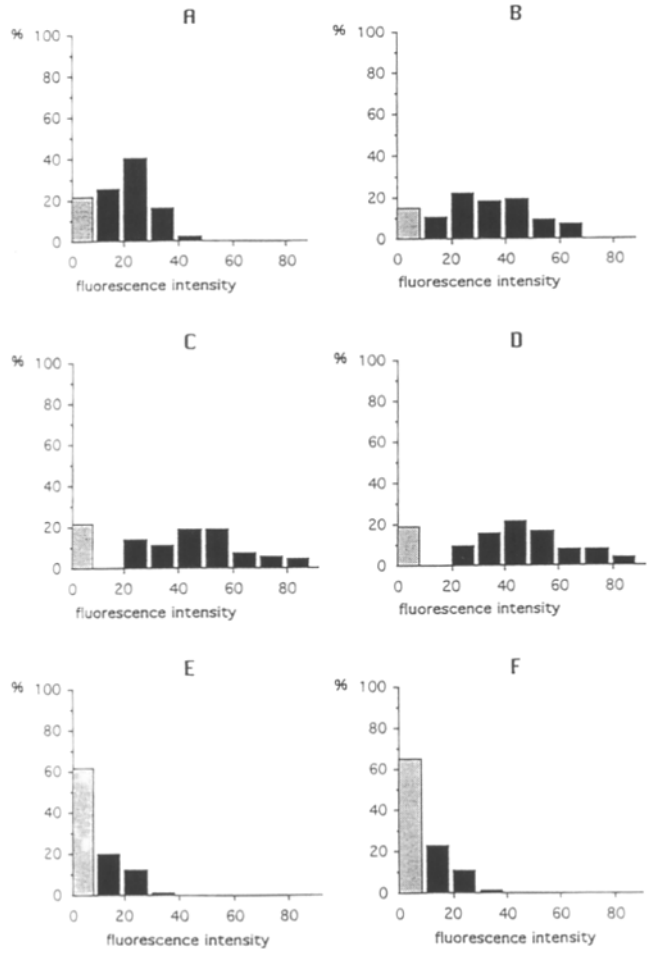

Figure 10. GTP-γS stimulates actin polymerization in the buds of wild-type cells. Permeabilized DRL165-5a, wild-type (*A–D*) and DRL165-2a, *cdc42-1* (*E* and *F*) cells grown at 28°C were incubated with U buffer (*A*, *C*, and *E*) or U buffer containing 0.2 mM GTP-γS (*B*, *D*, and *F*) for 40 min at 30°C. Cells were washed with U buffer and were resuspended in 0.5 μM Rd-actin in U buffer containing 1 mM ATP. Cells were fixed after 4 min (*A*, *B*, *E*, and *F*) or 16 min (*C* and *D*) of incubation at 25°C. The distributions of incorporated levels of rhodamine fluorescence in the bud across the cell population are shown. The stippled bars represent the population of cells whose buds have the same background level of fluorescence as the mother cell.

(Fig. 11 *E*). Cdc42^{L61}p also shows a moderate effect on actin incorporation into the bud of wild-type cells (Fig. 11 *C*). These results suggest that Cdc42p plays a direct role in the regulation of polarized actin assembly.

Discussion

In vitro systems with physiological characteristics have proven invaluable for elucidating the molecular mechanisms underlying many biological processes (Swanson, 1993). This is especially true when biochemical analyses can be combined with genetic analyses, as has been done for the secretory pathway (Pryer et al., 1992). Because genetic analyses have implicated a large number of interacting genes in polarized cell growth and actin cytoskeleton organization, in vitro assays that can carry out crucial events during polarized cell growth, such as polarized actin cytoskeleton assembly, will be highly valuable in defining the biochemical function of these individual gene products, as well as elucidating the biochemical mechanisms of cell polarity establishment. Here we have reported the establishment of an in vitro assay in which actin assembly occurs at the cortex of permeabilized yeast cells. Several lines of evidence suggest strongly that the assembly of actin in permeabilized yeast cells occurs in a physiologically relevant manner. First, we have chosen for our studies to concentrate on small-budded cells because, as the surface area of the growing buds of these cells increases rapidly (at 30°C, the surface area of a small bud must increase 5- to 10-fold in ~30 min), the actin cytoskeleton that underlies the plasma membrane of the entire bud surface, but not the mother cell surface, must be undergoing rapid assembly. Thus, when we quickly freeze and permeabilize this population of cells, it is most likely that exogenously added fluorescent actin will assemble at the sites where assembly occurs in vivo. Second, actin assembly in the cells permeabilized during bud growth occurs at discreet cortical sites that are located predominantly in the developing bud, a pattern that closely reflects the in vivo distribution of actin patches. Third, the Rd-actin incorporation pattern always reflects the cell cycle stage of the permeabilized cells. For example, many large-budded cells with divided nuclei incorporate Rd-actin into the region of septum formation rather than into the bud, consistent with the in vivo organization of actin during cytokinesis (Kilmartin and Adams, 1984). Fourth, Δ*sla1*, Δ*sla2*, and *cdc42-1* mutations that affect cellular actin distribution and polarized cell growth in vivo abolish Rd-actin incorporation in the permeabilized cells. Finally, Rd-actin incorporation in the bud of permeabilized cells does not result from trapping or nonspecific aggregation of fluorescent actin monomers at the cell surface, but it requires actin polymerization. Furthermore, this actin polymerization does not occur by nonspecific assembly of actin onto preexisting actin structures in the permeabilized cells because some of the actin patches assembled in vitro do not coincide with preexisting actin patches (Fig. 1). These patches may reflect new sites that have been activated for actin assembly at the time the cells are frozen.

Spatial Regulation of Actin Assembly during Polarized Cell Growth

The spatial pattern of actin assembly in the cell can in principle be regulated by controlling the availability of polymerizable actin monomers, the number and the distribution of nucleation sites, or by the selective stabilization of actin filaments (Stossel et al., 1989). The differential incorporation of Rd-actin in the bud versus the mother cell can not be ac-

Figure 9. In vitro actin assembly in mutants with defects in cytoskeleton components. DDY262, Δ*abp1* (A), DDY217, Δ*sac6* (B), DDY495, Δ*sla1* (C), and DDY496, Δ*sla2* (D) cells that had been grown at 25°C were permeabilized and incorporated Rd-actin for 8 min under conditions described in Materials and Methods. The left panels show phase images, and the right panels show rhodamine fluorescence images. Bar, 10 μm.

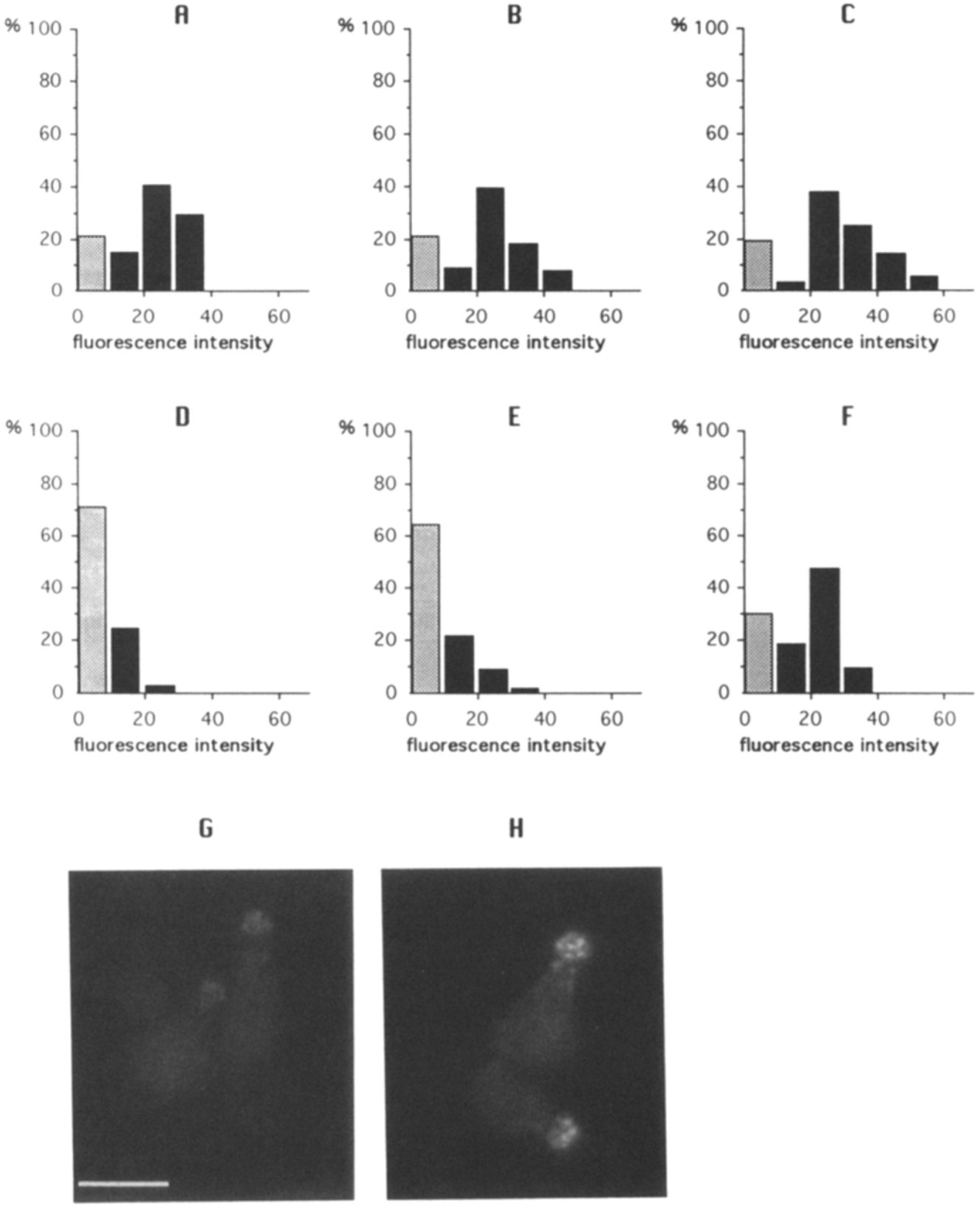

Figure 11. An activated Cdc42 protein restores actin nucleation activity in *cdc42-1* mutant cells. Permeabilized wild-type (*A–C*) and *cdc42-1* (*D–F*) cells grown at 28°C were incubated with 12 μl of U buffer + 8 μl Cdc42 buffer (20 mM Tris-HCl pH 8.0, 10 mM $MgCl_2$, 100 mM NaCl, 2% glycerol) (*A* and *D*), or + 8 μl Cdc42 buffer containing 0.1 mg/ml Cdc42-GDP (*B* and *E*) or 0.1 mg/ml $Cdc42^{L61}$-GTP (*C* and *F*) for 30 min at 30°C. Cells were washed and resuspended in 0.5 μM Rd-actin in U buffer containing 1 mM ATP. The reaction was terminated after 4 min of incubation at 25°C. The distributions of the levels of incorporated rhodamine fluorescence in the bud across the cell population are shown. The stippled bars represent the population of cells whose bud has the same background level of fluorescence as the mother cell. (*G* and *H*) Rhodamine fluorescence of representative cells from *D* and *F*, respectively. Bar, 10 μm.

counted for by the first mechanism since exogenous actin monomers are supplied uniformly throughout the cell as suggested by the uniform uptake of 70 kD fluorescein-dextran. Because actin incorporation in the bud does not have the lag phase characteristic of spontaneous filament formation, we conclude that the activity that promotes actin assembly in the bud facilitates the nucleation step.

Studies in various cell types such as fibroblasts and leukocytes have shown that free barbed ends of existing filaments are a common source of nucleation sites for actin polymerization. In detergent-permeabilized fibroblasts, an actin nucleation activity that is inhibited by barbed-end capping agents is located at the tips of lamellipodia (Symons and Mitchison, 1991). The activity that promotes actin incorporation into permeabilized neutrophils also appears to be provided by the barbed ends of existing filaments (Redmond and Zigmond, 1993). However, the nucleation activity in the permeabilized yeast cells is not inhibited by cytochalasin D treatment under conditions that block filament assembly from control yeast actin filaments. The fact that the nucleation activity in Δ*cap2* cells is sensitive to the CD treatment suggests that CD is active toward the endogenous yeast actin filament ends (Fig. 8 *B*). Nor could the activity be blocked by gelsolin, a barbed end-capping protein (Stossel et al., 1985; data not shown). Furthermore, the nucleation activity is completely abolished by a protease treatment that does not degrade the endogenous actin (Fig. 6 *A*). These results suggest that protein factors other than the barbed ends of actin filaments are responsible for nucleating actin assembly in the bud. However, this conclusion will not be definitive until the molecular components of the nucleation activity are identified.

One cytoskeletal protein that has been reported to nucleate actin filament formation is talin, a peripheral membrane protein that links actin filaments to focal adhesions (Kaufmann et al., 1991; Isenberg and Goldmann, 1992). The yeast protein Sla2 contains a COOH-terminal domain with significant sequence homology to talin (Holtzman et al., 1993). Disruption of *SLA2* is not lethal, but it causes a severe defect in polarized growth. We have shown that permeabilized Δ*sla2* cells fail to nucleate actin assembly in vitro, and this defect is not caused by a lack of permeability or by a difference in the cell cycle stage. Although we have not demonstrated that the effect of Δ*sla2* mutation is direct, the fact that Sla2p is localized in the cortical actin patches (Yang, S., and D. Drubin, unpublished results) is consistent with the possibility that Sla2p is a component of the actin nucleation sites. Another mutation that abolishes in vitro actin assembly is Δ*slal*. Like *sla2* mutations, *slal* mutations were isolated in a screen for mutations that exhibit synthetic lethality with Δ*abpl*. In an *ABP1* background, these mutations result in defects in polarized growth. The Slal protein contains three SH3 domains and, like Abpl and Sla2 proteins, is also localized in actin patches (Lila, T., and D. Drubin, unpublished results). If Slalp and Sla2p are required for nucleating actin assembly in the bud, how would one explain the facts that the F-actin content in Δ*slal* and Δ*sla2* cells appear to be similar to that in the wild-type cells, and that these mutants can actually form buds (Holtzman et al., 1993)? It is possible that in vivo the Δ*slal* and Δ*sla2* mutations only lead to a partial loss of the nucleation activity, and this defect can be partially compensated for by filament-binding proteins such as Abpl and Sac6. Synthetic lethal interactions between null alleles of *SLA1* and *ABP1*, of *SLA2* and *ABP1*, and of *SLA2* and *SAC6*, are in agreement with this hypothesis (Holtzman et al., 1993).

Rd-actin assembly in the bud of the permeabilized cells is saturable. This saturation is not caused by the depletion of the monomer pool by spontaneous filament formation outside the cells, or a time-dependent loss of permeability or actin assembly sites, because permeabilized cells that have been incubated in the buffer for 40 min can still incorporate Rd-actin efficiently (Fig. 10 *A*). A more likely explanation for the saturation is that the extent of filament assembly is restricted by the cell cortex, a possibility that is in agreement with the ultrastructural images of actin patches showing that fingerlike plasma membrane invaginations are surrounded by ordered arrays of actin (Mulholland et al., 1994). If this is true, how might the length of the actin filaments be controlled? Since proteins that nucleate actin assembly such as ponticulin and talin are also filament binding proteins (Luna et al., 1990; Muguruma et al., 1990; Goldmann and Isenberg, 1991; Kaufman et al., 1991), it is possible that similar proteins nucleate actin assembly in the bud and bind along the length of the filaments. This binding allows other protein factors localized in the cortical patches, such as capping protein or the actin severing protein cofilin (Amatruda and Cooper, 1992*a*; Moon et al., 1993), to control the length of these filaments. This model is supported by the observation that a mutant that lacks Cap2, a component of the yeast capping protein, incorporates actin to a much greater extent than wild-type cells. Δ*cap2* mutant cells also display a faster rate of Rd-actin incorporation, probably because of an increase in the number of nucleation sites contributed by the uncapped barbed ends of endogenous filaments.

The Role of Small GTP-binding Proteins in Regulating Actin Assembly

Changes in cell morphology occur either according to inherited instructions or in response to external signals. Studies of the molecular pathways that lead to cytoskeletal changes during cellular morphogenesis in a variety of cell types have revealed that small Ras-like GTP-binding proteins play important but still undefined roles (reviewed in Hall, 1992). For example, microinjection of Rho into fibroblasts stimulates stress fiber formation. Conversely, inactivation of Rho blocks this process (Ridley and Hall, 1992). Using the permeabilized cell model, we tested the possibility that GTP-binding proteins directly control actin assembly. We demonstrated that permeabilized yeast cells that have been incubated with GTP-γS exhibit higher levels of actin nucleation activity than untreated cells. The most likely explanation for this result is that a GTP-binding protein in its GTP-bound form stimulates the nucleation activity. Because cytoplasmic proteins are presumably extracted during the permeabilization procedure, the action of the GTP-binding protein is probably not mediated through soluble factors, implying that the GTP-binding protein exerts its effects by interactions proximal to the sites of actin assembly.

One candidate for the GTP-binding protein that mediates the GTP-γS effect is Cdc42, a protein required for yeast polarized growth (Adams et al., 1990). Cdc42 is a prenylated protein that has been immunolocalized to the cell cor-

tex mainly in the growing bud (Ziman et al., 1993). Localization of Cdc42p by immunoelectron microscopy shows that Cdc42p staining is most pronounced in plasma membrane invaginations, where cortical actin is also found (Ziman et al., 1993). We demonstrated that *cdc42-1* cells grown at 28°C, a temperature at which the cells show some defects in apical growth, exhibit a reduced level of the nucleation activity, and that this nucleation activity is not stimulated by GTP-γS (Fig. 10). Furthermore, the loss of actin nucleation activity in *cdc42-1* mutant cells grown at 28°C can be complemented in vitro by a purified constitutively active Cdc42 protein, but not by the GDP-bound wild-type Cdc42 protein (Fig. 11). Together, these results suggest that Cdc42p, in its GTP-bound form, stimulates actin filament assembly by interacting directly with the components of the actin nucleation sites.

We thank Tim O'Connor, Rick Cerione, Christine Field, Kent McDonald, and Marc Kirschner for valuable help and advice; John Cooper and Yoshikazu Ohya for providing mutant yeast strains; and Doug Holtzman and Anne Moon for providing yeast actin. We are grateful to Kathryn Ayscough, Marc Kirschner, Tim Mitchison, Anne Moon, and Andrew Murray for their comments on the manuscript.

This work was supported by grants to David Drubin from the National Institute of General Medical Sciences (GM-42759), the American Cancer Society (CB-106), and the Searle Scholar Program/the Chicago Community Trust. Rong Li is a fellow of the Damon Runyon-Walter Winchell Cancer Research Foundation.

Received for publication 8 September 1994 and in revised form 13 November 1994.

References

Adams, A. E. M., D. Botstein, and D. G. Drubin. 1989. A yeast actin-binding protein is encoded by *SAC6*, a gene found by suppression of an actin mutation. *Science (Wash. DC).* 243:231–233.

Adams, A. E. M., D. I. Johnson, R. M. Longnecker, B. F. Sloat, and J. R. Pringle. 1990. *CDC42* and *CDC43*, two additional genes involved in budding and the establishment of cell polarity in the yeast *Saccharomyces cerevisiae*. *J. Cell Biol.* 111:131–142.

Amatruda, J. F., J. F. Cannon, K. Tatchell, C. Hug, and J. A. Cooper. 1990. Disruption of the actin cytoskeleton in yeast capping protein mutants. *Nature (Lond.).* 344:352–354.

Amatruda, J. F., and J. A. Cooper. 1992*a*. Purification, characterization, and immunofluorescence localization of *Saccharomyces cerevisiae* capping protein. *J. Cell Biol.* 117:1067–1076.

Amatruda, J. F., D. J. Gattermeir, T. S. Karpova, and J. A. Cooper. 1992*b*. Effects of null mutations and overexpression of capping protein on morphogenesis, actin distribution, and polarized secretion in yeast. *J. Cell Biol.* 119:1151–1162.

Bender, A., and J. R. Pringle. 1989. Multicopy expression of the *cdc24* budding defect in yeast by *CDC24* and the three newly identified genes including the *ras*-related gene *RSR1*. *Proc. Natl. Acad. Sci. USA.* 86:9976–9980.

Bretscher, A. 1991. Microfilament structure and function in the cortical cytoskeleton. *Annu. Rev. Cell Biol.* 7:337–374.

Brown, S. S., and J. A. Spudich. 1981. Mechanism of action by cytochalasin: evidence that it binds to actin filaments. *J. Cell Biol.* 88:487–491.

Chant, J., K. Corrado, J. R. Pringle, and I. Herskowitz. 1991. Yeast *BUD5*, encoding a putative GDP-GTP exchange factor, is necessary for bud site selection and interacts with bud formation gene *BEM1*. *Cell.* 65:1213–1224.

Chant, J., and I. Herskowitz. 1991. Genetic control of bud site selection in yeast by a set of gene products that constitute a morphogenetic pathway. *Cell.* 65:1203–1212.

Chowdhury, S., K. W. Smith, and M. C. Gustin. 1992. Osmotic stress and the yeast cytoskeleton: phenotype-specific suppression of an actin mutation. *J. Cell Biol.* 118:561–571.

Drubin, D. G., K. G. Miller, and D. Botstein. 1988. Yeast actin-binding proteins: evidence for a role in morphogenesis. *J. Cell Biol.* 107:2551–2561.

Estes, J. E., L. A. Selden, and L. C. Gershman. 1981. Mechanisms of action of phalloidin on the polymerization of muscle actin. *Biochemistry.* 20: 708–712.

Ford, S., and J. Pringle. 1986. Development of spatial organization during the formation of zygotes and shmoos in *Saccharomyces cerevisiae*. *Yeast.* 2:S114.

Goldmann, W. H., and G. Isenberg. 1991. Kinetic determination of talin-actin binding. *Biochem. Biophys. Res. Commun.* 178:718–723.

Hall, A. 1992. Ras-related GTPases and the cytoskeleton. *Mol. Biol. Cell.* 3:475–479.

Holtzman, D. A., S. Yang, and D. G. Drubin. 1993. Synthetic-lethal interactions identify two novel genes, *SLA1* and *SLA2*, that control membrane cytoskeleton assembly in *Saccharomyces cerevisiae*. *J. Cell Biol.* 122:635–644.

Holtzman, D. A., K. F. Wertman, and D. G. Drubin. 1994. Mapping actin sufaces required for functional interactions in vivo. *J. Cell Biol.* 126:423–432.

Isenberg, G., and W. H. Goldmann. 1992. Actin-membrane coupling: a role for talin. *J. Muscle Res. Cell Motil.* 13:587–589.

Johnson, D. I., and J. R. Pringle. 1990. Molecular characterization of *CDC42*, a *Saccharomyces cerevisiae* gene involved in the development of cell polarity. *J. Cell Biol.* 111:143–52.

Kaufmann, S., T. Piekenbrock, W. H. Goldmann, M. Bärmann, and G. Isenberg. 1991. Talin binds to actin and promotes filament nucleation. *FEBS (Fed. Eur. Biochem. Soc.) Letters.* 284:187–191.

Kellogg, D. R., T. J. Mitchison, and B. M. Alberts. 1988. Behavior of microtubules and actin filaments in living *Drosophila* embryos. *Development (Camb.).* 103:675–686.

Kilmartin, J., and A. E. M. Adams. 1984. Structural rearrangements of tubulin and actin during the cell cycle of the yeast *Saccharomyces*. *J. Cell Biol.* 98:922–933.

Lowry, O. H., N. J. Rosebrough, A. L. Farr, and R. J. Randal. 1951. Protein measurement with the Folin phenol reagent. *J. Biol. Chem.* 3:265–275.

Luna, E. J., C. P. Wuestehube, C. P. Chia, A. Shariff, A. L. Hitt, and H. M. Ingalls. 1990. Ponticulin, a developmentally regulated plasma membrane glycoprotein, mediates actin binding and nucleation. *Dev. Genet.* 11: 354–361.

Moon, A. L., P. A. Janmey, K. A. Louie, and D. G. Drubin. 1993. Cofilin is an essential component of the yeast cortical cytoskeleton. *J. Cell Biol.* 120:421–435.

Muguruma, M., S. Matsumura, and T. Fukazawa. 1990. Direct interactions between talin and actin. *Biochem. Biophys. Res. Commun.* 171:1217–1223.

Mulholland, J., D. Preuss, A. Moon, A. Wong, D. Drubin, and D. Botstein. 1994. Ultrastructure of the yeast actin cytoskeleton and its association with the plasma membrane. *J. Cell Biol.* 125:381–392.

Pardee, J. D., and J. A. Spudich. 1982. Purification of muscle actin. *Methods Enzymol.* 85:164–181.

Pollard, T. D., and S. W. Craig. 1982. Mechanism of actin polymerization. *Trends Biochem. Sci.* 7:55–58.

Pollard T. D. 1984. Polymerization of ADP-actin. *J. Cell Biol.* 99:769–777.

Pollard, T. D. 1986. Rate constants for the reactions of ATP and ADP actin with the ends of actin filaments. *J. Cell Biol.* 103:2747–2754.

Pollard, T. D., and J. A. Cooper. 1986. Actin and actin binding proteins. A critical evaluation of mechanisms and functions. *Annu. Rev. Biochem.* 55:987–1035.

Pringle, J. R., R. A. Preston, A. E. Adams, T. Stearns, D. G. Drubin, B. K. Haarer, and E. W. Jones. 1989. Fluorescence microscopy methods for yeast. *Methods Cell Biol.* 31:357–435.

Pryer, N. K., L. J. Wuestehube, and R. Schekman. 1992. Vesicle-mediated protein sorting. *Annu. Rev. Biochem.* 61:471–516.

Redmond, T., and S. H. Zigmond. 1993. Distribution of F-actin elongation sites in lysed polymorphonuclear leukocytes parallel the distribution of endogenous actin. *Cell Motil. Cytoskeleton.* 26:7–18.

Reed, E. B., H. H. Okamura, and D. G. Drubin. 1992. Actin- and tubulin-dependent functions during *Saccharomyces cerevisiae* mating projection formation. *Mol. Biol. Cell.* 3:429–444.

Ridley, A. J., and A. Hall. 1992. The small GTP-binding protein Rho regulates the assembly of focal adhesions and actin stress fibers in response to growth factors. *Cell.* 70:389–399.

Ridley, A. J., H. F. Paterson, C. L. Johnston, D. Diekmann, and A. Hall. 1992. The small GTP-binding protein Rac regulates growth factor–induced membrane ruffling. *Cell.* 70:401–410.

Shefcyk, J., M. Yassin, T. F. P. Volpi, P. H. Molsky, and J. J. Naccache. 1985. Pertussis toxin but not cholera toxin inhibits the stimulated increase in actin association with the cytoskeleton in rabbit neutrophils: role of the "G-proteins" in stimulus-response coupling. *Biochem. Biophys. Res. Commun.* 26:1174–1181.

Sherman, F., G. R. Fink, and J. B. Hicks. 1974. Methods in Yeast Genetics. Cold Spring Harbor Laboratory Press, Cold Spring Harbor, NY. 186 pp.

Shortle, D., J. E. Haber, and D. Botstein. 1982. Lethal disruption of the yeast actin gene by integrative DNA transformation. *Science (Wash. DC).* 217:371–373.

Sloat, B. F., A. E. M. Adams, and J. R. Pringle. 1981. Roles of the *CDC24* gene product in cellular morphogenesis during the *Saccharomyces cerevisiae* cell cycle. *J. Cell Biol.* 89:395–405.

Stossel, T. P., C. Chaponnier, R. M. Ezzell, J. H. Hartwig, P. A. Janmey, D. J. Kwiastkowski, S. E. Lind, D. B. Smith, H. L. Southwick, H. L. Yin. 1985. Nonmuscle actin binding proteins. *Annu. Rev. Cell Biol.* 1:353–402.

Stossel, T. 1989. From signal to pseudopod. *J. Biol. Chem.* 264:18261–18264.

Swanson, J. A. 1993. Pure thoughts with impure proteins: permeabilized cell

models of organelle motility. *Bioessays.* 15:715–722.
Symons, M. H., and T. J. Mitchison. 1991. Control of actin polymerization in live and permeabilized fibroblasts. *J. Cell Biol.* 114:503–13.
Welch, M. D., D. A. Holtzman, and D. G. Drubin. 1994. The yeast actin cytoskeleton. *Curr. Opin. Cell Biol.* 6:110–119.
Zheng, Y., R. Cerione, and A. Bender. 1994. Control of the yeast bud-site assembly GTPase Cdc42. *J. Biol. Chem.* 269:2369–2372.
Ziman, F., J. M. O'Brien, L. A. Ouellette, W. R. Church, and D. I. Johnson. 1991. Mutational analysis of *CDC42Sc*, a *Saccharomyces cerevisiae* gene that encodes a putative GTP-binding protein involved in the control of cell polarity. *Mol. Cell. Biol.* 11:3537–3544.
Ziman, M., D. Preuss, J. Mulholland, J. M. O'Brien, D. Botstein, and D. I. Johnson. 1993. Subcellular localization of Cdc42p, a *Saccharomyces cerevisiae* GTP-binding protein involved in the control of cell polarity. *Mol. Biol. Cell.* 4:1307–1316.